Design of Impulsive Feedback Controller for Dosing

Design of Impulsive Feedback Controller for Dosing

Alexander Medvedev[1], Anton V. Proskurnikov[2], and Zhanybai T. Zhusubaliyev[3,4]

***Abstract*— This paper proposes a pulse-modulated controller that generates, under stationary conditions, a desired sequence of uniform and equidistant impulsive control actions from continuous measurements of the output of a smooth nonlinear time-invariant positive single-input single-output plant of Wiener structure. The proposed controller is applied to the dosing of the drug *atracurium* in closed-loop neuromuscular blockade and its performance is studied on a database of patient-specific pharmacokinetic-pharmacodynamic models previously estimated from clinical data.**

I. Introduction

An everyday life example of a dosing application is following doctor's orders on medication regimen, for instance, "take one tablet twice a day". This is an open-loop dosing strategy that does not consider the medication effect in the particular patient. Further, increasing or decreasing the amount of each single dose corresponds to the mechanism of amplitude modulation in pulse-modulated control [1] whereas manipulating the dosing interval constitutes the principle of frequency modulation.

Besides pharmacotherapies, where drugs are administered in tablet or injection form, similar dosing problems characterized by (relatively rare) impulsive control action and continuous measurement of the effect are commonly found in space technology, water treatment, food, chemical and biochemical industries, agriculture, steel and mining industries, to name a few. An industrial dosing control system is typically open-loop and implemented by means of discrete logic or automata [2]. An early example of applying optimal control to dosing is the work of R. Bellman in [3]. However, the open-loop control cannot neither attenuate disturbances nor handle plant uncertainty. Motivated by a drug-dosing application and an available pharmacokinetic-pharmacodynamic (PK/PD) model, a Model-Predictive Control (MPC) with impulsive control action was proposed in [4].

Notably, physiological and, in particular, endocrine regulation in a living organism is often performed in an impulsive manner. The physiological profile of insulin secretion is around ten major hormone pulses over 24 hours [5] with their temporal distribution related to meals. A promising application of impulsive MPC approach to insulin dosing in simulated diabetes patients is reported in e.g. [6].

Impulsive feedback control is inherently nonlinear and adding an advanced control law, such as MPC, to the closed-loop dynamics further complicates stability and performance analysis. Yet, simple pulse-modulated feedback solutions manipulating the amplitude and frequency of the control impulses have been lacking until recently. In [7], [8], it is suggested that a nonlinear amplitude and frequency pulse modulator can be designed to control a positive continuous linear time-invariant third-order plant to a given periodic solution through localization of the multipliers of the fixed point of the closed-loop system. This paper employs the concept of pulse-modulated feedback control and examines its feasibility and performance limitations with respect to a dosing application in neuromuscular blockade (NMB).

The main contributions of the paper are as follows. First, for the nonlinear PK/PD model at hand, a closed-form expression for the fixed point defining the stationary dosing solution is obtained. Second, for a population of PK/PD models previously estimated from clinical data, the achievable convergence rates under amplitude or frequency modulation feedback alone are established. Third, it is demonstrated that the parameters of the modulation functions that yield best convergence can be calculated from the Hopf bifurcation points that the desired stationary solution undergoes.

II. Neuromuscular blockade model

A continuous-time Wiener model for NMB with the muscle relaxant *atracurium* under general closed-loop anesthesia is introduced in [9]. The model assumes continuous infusion of the drug and the input $u(t)$ is the administered atracurium rate in $[\mu\text{g kg}^{-1}\text{min}^{-1}]$, positive and bounded. The current NMB level constitutes the model output $y(t)$ $[\%]$ and is measured by a train-of-four monitor (peripheral nerve stimulator). When the NMB is initiated and there is no drug in the bloodstream, the output is maximized, i.e. $y(t) = 100\%$.

The PK part is described by a transfer function with a unit static gain, whose pole spectrum scales linearly with α

$$W(s) = \frac{\bar{Y}(s)}{U(s)} = \frac{v_1 v_2 v_3 \alpha^3}{(s + v_1\alpha)(s + v_2\alpha)(s + v_3\alpha)}, \qquad (1)$$

where $\bar{Y}(s) = \mathcal{L}\{\bar{y}(t)\}$, $U(s) = \mathcal{L}\{u(t)\}$, and $\mathcal{L}\{\cdot\}$ denotes the Laplace transform. The parameter $0 < \alpha \leq 0.1$ is estimated from patient-specific data, whereas the other parameters in (1) are estimated from cohort data and fixed (see [9]), $v_1 = 1$, $v_2 = 4$, and $v_3 = 10$. The PD part of

Alexander Medvedev [alexander.medvedev@it.uu.se] is with Department of Information Technology, Uppsala University, SE-752 37 Uppsala, Sweden.

Anton V. Proskurnikov [anton.p.1982@ieee.org] is with Department of Electronics and Telecommunications, Politecnico di Torino, Turin, Italy, 10129.

Zhanybai T. Zhusubaliyev [zhanybai@hotmail.com] is with Department of Computer Science, International Scientific Laboratory for Dynamics of Non-Smooth Systems, Southwest State University, Kursk, Russia and Faculty of Mathematics and Information Technology, Osh State University, Lenin st. 331, 723500, Osh, Kyrgyzstan.

the NMB model is static and relates the output $\bar{y}(t)$ to the measured effect $y(t)$ by the Hill-type function

$$y(t) = \varphi(\bar{y}(t)) \triangleq \frac{100C_{50}^{\gamma}}{C_{50}^{\gamma} + \bar{y}^{\gamma}(t)}, \tag{2}$$

where $C_{50} = 3.2425$ μg ml^{-1} is the drug concentration producing 50% of the maximum effect and $0 < \gamma \leq 10$ is a patient-specific parameter. In (1), (2), the effect of the NMB agent on the patient is captured with the pair (α, γ).

III. Problem formulation

Consider the following realization of model (1), (2)

$$\dot{x}(t) = Ax(t) + Bu(t),\ \bar{y}(t) = Cx(t),\ y(t) = \varphi(\bar{y}(t)), \tag{3}$$

where $x = [x_1, x_2, x_3]^{\top}$,

$$A = \begin{bmatrix} -a_1 & 0 & 0 \\ g_1 & -a_2 & 0 \\ 0 & g_2 & -a_3 \end{bmatrix}, B = \begin{bmatrix} 1 \\ 0 \\ 0 \end{bmatrix}, C^{\top} = \begin{bmatrix} 0 \\ 0 \\ 1 \end{bmatrix},$$

and $a_1 = v_1\alpha$, $a_2 = v_2\alpha$, $a_3 = v_3\alpha$, $g_1 = v_1\alpha$, $g_2 = v_2v_3\alpha^2$.

It is readily observed that the matrix A is Hurwitz stable and Metzler. The nonlinear function $\varphi(\cdot)$ is smooth, positive, and bounded. Asymptotic stability of (3) agrees well with the fact that chemical substances decay with time and the (element-wise) positivity of x ensures an interpretation of the state variables in terms of (compartment) concentrations. The chain structure of (3) portrays dynamics of three substances' concentrations, where a preceding substance stimulates the production of the next one.

Let continuous plant (3) be controlled by an output feedback that constitutes a frequency and amplitude pulse modulation operator [1]. Then the impulsive control law is given by the first-order difference equation

$$\begin{aligned} x(t_n^+) = x(t_n^-) + \lambda_n B, \quad t_{n+1} = t_n + T_n, \\ T_n = \bar{\Phi}(y(t_n)), \quad \lambda_n = \bar{F}(y(t_n)), \end{aligned} \tag{4}$$

where $n = 0, 1, \ldots$ The minus and plus in a superscript in (4) denote the left-sided and a right-sided limit, respectively. The instants t_n are called (impulse) firing times and λ_n represents the corresponding impulse weight. Then, the impulsive controller degrees of freedom are the frequency modulation function $\bar{\Phi}(\cdot)$ and the amplitude modulation function $\bar{F}(\cdot)$. Despite the jumps in (4), y is a smooth function since

$$CB = 0,\ CAB = 0,\ CA^2B \neq 0. \tag{5}$$

With $\circ$ denoting composition, introduce the functions

$$\Phi(\cdot) \triangleq (\bar{\Phi} \circ \varphi)(\cdot), \quad F(z\cdot) \triangleq (\bar{F} \circ \varphi)(\cdot).$$

In order to obtain a stabilizing feedback, both $F(\cdot)$ and $\Phi(\cdot)$ have to be continuous and monotonic, $F(\cdot)$ be non-increasing, and $\Phi(\cdot)$ be non-decreasing. To guarantee boundedness of closed-loop solutions in (3), (4), it is required that

$$0 < \Phi_1 \leq \Phi(\cdot) \leq \Phi_2, \quad 0 < F_1 \leq F(\cdot) \leq F_2, \tag{6}$$

where Φ_1, Φ_2, F_1, F_2 are constants.

The control problem at hand is then to select the modulation functions $\bar{\Phi}(\cdot)$, $\bar{F}(\cdot)$ so that closed-loop system (3), (4) exhibits an orbitally stable periodic solution with predefined amplitude and period $\forall n : \lambda_n = \lambda, T_n = T$.

In terms of the NMB model introduced in Section II, the sought impulsive controller administers, under stationary conditions, a dose of λ μg of atracurium each T minutes. When disturbed within the basin of attraction, the solution of (3), (4) returns to the designed stationary periodic solution.

IV. System dynamics

With the plant nonlinearity φ incorporated in the modulation functions Φ and F, closed-loop system (3),(4) constitutes the Impulsive Goodwin's Oscillator (IGO) [10], [11], a hybrid mathematical model originally devised to describe pulsatile endocrine regulation. Denoting $X_n = x(t_n^-)$, the state vector sequence of the of the IGO obeys the map [11]

$$\begin{aligned} X_{n+1} &= Q(X_n), \\ Q(\xi) &= \mathrm{e}^{A\Phi(C\xi)}\left(\xi + F(C\xi)B\right). \end{aligned} \tag{7}$$

In between the impulsive feedback firings t_n and t_{n+1}, the continuous state trajectory is uniquely defined by X_n as

$$x(t) = \mathrm{e}^{(t-t_n)A}(X_n + \lambda_n B), \quad t \in (t_n, t_{n+1}). \tag{8}$$

A periodic solution of the IGO with one firing of the feedback in the period is referred to as 1-cycle [12]. For such a solution, $\forall n : X_n = X$, where X is a solution to

$$X = Q(X). \tag{9}$$

As proved in [11], (9) always has a unique solution $X > 0$ constituting the fixed point that completely defines a 1-cycle. The Jacobian of map $Q(\cdot)$ at the point X is given by [7]

$$\begin{aligned} Q'(X) &= \mathrm{e}^{A\Phi(\bar{y}_0)} + (F'(\bar{y}_0)J + \Phi'(\bar{y}_0)D)\,C, \\ \bar{y}_0 &\triangleq CX,\ D \triangleq AX,\ J = \mathrm{e}^{A\Phi(\bar{y}_0)}\,B. \end{aligned} \tag{10}$$

The 1-cycle corresponding to the fixed point X is orbitally stable when the matrix $Q'(X)$ is Schur [11].

Now the control problem defined in the end of the previous section can be reformulated in terms of the fixed point. Given the plant in (3) and the desired parameters of the periodic solution λ and T, find the modulation functions $\bar{\Phi}(\cdot)$ and $\bar{F}(\cdot)$ such that the fixed point X satisfying (9) also solves the equations $\Phi(\bar{y}_0) = T$, $F(\bar{y}_0) = \lambda$ and renders the matrix $Q'(X)$ Schur-stable.

The selection of $F'(z_0), \Phi'(z_0)$ to stabilize the fixed point X is equivalent to finding K that renders the matrix

$$Q'(X) = A_{\Phi} + WKC \tag{11}$$

Schur-stable, where

$$A_{\Phi} = \mathrm{e}^{A\Phi(z_0)}, W = \begin{bmatrix} J & D \end{bmatrix}, K^{\top} = \begin{bmatrix} F'(z_0) & \Phi'(z_0) \end{bmatrix}.$$

As demonstrated in [13],

$$JF'(\bar{y}_0) + D\Phi'(\bar{y}_0) < 0, \tag{12}$$

for all feasible values of $F'(\bar{y}_0), \Phi'(\bar{y}_0)$. Inequality (12) highlights the role of pulse-modulated feedback (4) as a negative feedback with respect to the output $\bar{y}(t)$, [7].

V. Data set

The data set used in this study is described in detail in [9]. The model parameter estimates for 48 patients are illustrated in Fig. 1. The correlation between the estimates of α and γ is low. Notice that the models with extreme values of γ do not exhibit high values of α as well as high values of both parameters do not occur at all. On the contrary, the model with Patient Identification Number (PIN) 26 exhibits the least value of γ and the largest value of α. It is unclear whether this a biologically motivated phenomenon or an artifact contributed by the model estimation technique.

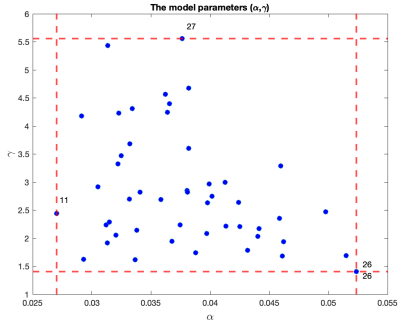

Fig. 1. The model parameter pairs in the data set. $0.0270 \leq \alpha \leq 0.0524$, $1.4030 \leq \gamma \leq 5.5619$. The extreme parameter values are indicated by the Patient Identification Number.

VI. Impulsive controller design

A design procedure to solve the posed impulsive control problem has to produce a fixed point satisfying the parameters of the desired 1-cycle and ensure its stability by the choice of the modulation functions. Further, one seeks to obtain fast and non-oscillating convergence to the stationary solution under a perturbation of the initial conditions.

A. Fixed point

Introduce a first divided difference of a function $h(\cdot)$

$$h[x_1, x_2] \triangleq \frac{h(x_1) - h(x_2)}{x_1 - x_2},$$

and higher-order divided differences defined recursively by

$$h[x_0, \ldots, x_k] = \frac{h[x_1, \ldots, x_k] - h[x_0, \ldots, x_{k-1}]}{x_k - x_0}.$$

Proposition 1: For model (1), (2) in the state-space form of (3) and exhibiting a 1-cycle of the period T with the weight λ, the fixed point satisfying (9) is given by

$$X = \lambda \begin{bmatrix} \mu(-\alpha v_1) \\ \alpha v_1 \mu[-\alpha v_1, -\alpha v_2] \\ \alpha^3 v_1 v_2 v_3 \mu[-\alpha v_1, -\alpha v_2, -\alpha v_3] \end{bmatrix}, \qquad (13)$$

where $\mu(x) = \frac{1}{\mathrm{e}^{-Tx} - 1}$.

Proof: Omitted for brevity. ■

Naturally, a vector X can be obtained from (13) even though a 1-cycle is not observed in closed-loop system (3), (4). As proven in [11], 1-cycle always exists but does not have to be stable.

B. Stability

To sustain the desired periodical solution in closed-loop system (3), (4), 1-cycle has to be orbitaly stable which property is guaranteed by stability of the fixed point.

Actually, stability of the 1-cycle is readily achieved without impulsive feedback (4), i.e. with constant modulation functions $F(z) \equiv \lambda$, $\Phi(z) \equiv T$ (thus implying $K = 0$ in (11)) which is equivalent to driving (3) open-loop with a train of equidistant impulses with constant weights. The impulsive feedback is though instrumental in improving the convergence to the desired periodical solution under deviation. As (7) implies, without the feedback, the (local) convergence is determined by the spectral radius of e^{AT} that is always less than one, due to A being Hurwitz. Recalling (12), it also follows that increasing $\Phi'(z_0)$ and decreasing $F'(z_0)$ leads to a larger spectral radius of $Q'(X)$ and, eventually, loss of fixed point stability. Then, another type of periodic solutions arises. Since the standard bifurcation mechanism in the IGO is frequency doubling [14], a stable 2-cycle typically emerges when a 1-cycle loses stability.

A numerically calculated illustration of 1-cycle stability is provided in Fig. 2. The spectral radius $\rho(Q'(X))$ is more sensitive to $\Phi'(z_0)$ than to $F'(z_0)$. Therefore, manipulating the dose administration time by means of frequency modulation is more potent way of controlling the plant than dose adjustment, i.e. amplitude modulation.

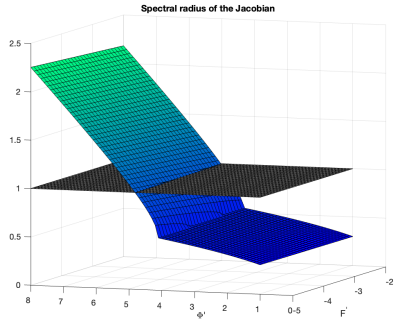

Fig. 2. Spectral radius $\rho(Q'_F(X))$ as function of $F'(z_0)$ and $\Phi'(z_0)$. The stability border is depicted by the crossing of the colored and grey plane. The mean population value of α is used.

Notably, the Jacobian only characterisers the dynamical behaviors of a linearization of (3),(4) in vicinity of the fixed point X. Then Fig. 2 reflects the stability properties of the linearized system that do not necessarily coincide with those of the underlying nonlinear dynamics.

C. Convergence rate

The eigenvalues of the Jacobian are as well the multipliers of the fixed point and, besides the convergence rate to the periodic solution, define the character of the transients. In dosing applications, it is desirable for a fixed point to possess positive multipliers as they render a (locally) monotone convergence of the desired solution. By making use of (10), the problem of minimizing the spectral radius of the Jacobian

by selecting K in (11) is

$$K^* = \arg\min_K \max_{i=1,\dots,3} |\xi_i \left(\mathrm{e}^{AT} + F'(\bar{y}_0)JC + \Phi'(\bar{y}_0)DC\right)|,$$

where $\xi(\cdot)$ denotes eigenvalue. The problem of minimizing the spectral radius of a non-symmetric affine matrix function is considered in e.g. [15]. It is non-convex and non-smooth as the eigenvalues are generally not differentiable.

a) Amplitude modulation: To obtain a better insight into the spectral properties of $Q'(\cdot)$ and how they depend on the impulsive controller, consider a special case of amplitude modulation that is obtained from (4) by letting $\Phi(z) \equiv T$. Then the Jacobian takes the form of

$$Q'_F(X) = \mathrm{e}^{AT} + F'(z_0)JC.$$

Here vector $J = \mathrm{e}^{AT}B$ is the first column of the matrix exponential, which can be found as follows [13]

$$\mathrm{e}^{At} = \begin{bmatrix} \mathrm{e}^{-a_1 t} & 0 & 0 \\ g_1 t\,\mathrm{e}[-a_1 t, -a_2 t] & \mathrm{e}^{-a_2 t} & 0 \\ g_1 g_2 t^2\,\mathrm{e}[-a_1 t, -a_2 t, -a_3 t] & g_2 t\,\mathrm{e}[-a_2 t, -a_3 t] & \mathrm{e}^{-a_3 t} \end{bmatrix}.$$

Proposition 2: Let ξ be a real eigenvalue of $Q'_F(X)$. A corresponding eigenvector is then given by

$$V = \begin{bmatrix} F'(z_0)\frac{\mathrm{e}^{-a_1 T}}{\mathrm{e}^{-a_1 T} - \xi} \\ F'(z_0)\xi\frac{g_1 T\,\mathrm{e}[-a_1 T, -a_2 T]}{(\mathrm{e}^{-a_1 T} - \xi)(\mathrm{e}^{-a_2 T} - \xi)} \\ 1 \end{bmatrix},$$

and the characteristic polynomial of $Q'_F(X)$ is

$$\mathcal{D}(s) = s^3 - \gamma_1 s^2 - \gamma_2 s - \gamma_3 = 0, \qquad (14)$$

where

$$\begin{aligned} \gamma_1 &= \mathrm{e}^{-a_1 T} + \mathrm{e}^{-a_2 T} + \mathrm{e}^{-a_3 T} \\ &\quad + F'(z_0) g_1 g_2 T^2\,\mathrm{e}[-a_1 T, -a_2 T, -a_3 T], \\ \gamma_2 &= F'(z_0) g_1 g_2 T^2 \left(\mathrm{e}[-a_1 T, -a_2 T]\,\mathrm{e}[-a_2 T, -a_3 T]\right. \\ &\quad \left. - \mathrm{e}^{-a_2 T}\,\mathrm{e}[-a_1 T, -a_2 T, -a_3 T]\right) - \\ &\quad - \mathrm{e}^{-(a_1+a_2)T} - \mathrm{e}^{-(a_1+a_3)T} - \mathrm{e}^{-(a_2+a_3)T}, \\ \gamma_3 &= \mathrm{e}^{-(a_1+a_2+a_3)T}. \end{aligned}$$

Proof: The proof is straightforward and omitted here. ■

The coefficients of characteristic polynomial (14) provide information on the eigenvalues of $Q'_F(X)$ since $\gamma_1 = \mathrm{Tr}\, Q'_F(X) = \sum_i^3 \xi_i$ and $\gamma_3 = \det Q'_F(X) = \prod_1^3 \xi_i$. Apparently, the product of the eigenvalues of the Jacobian is independent of the amplitude modulation feedback and a decrease in one of the eigenvalue will be accompanied with a rise in the other ones. The sum of the eigenvalues is an affine function of $F'(z_0)$. All the Jacobian eigenvalues are influenced by the amplitude modulation characteristic.

To maximize the convergence rate to the desired solution of the linearized at the fixed point closed-loop dynamics of (3),(4), one seeks for the value of $F'(z_0)$ that minimizes the spectral radius of $Q'_F(X)$. Fig. 3 shows the absolute values of the eigenvalues of $Q'_F(X)$ as function of $F'(z_0)$. The minimum spectral radius value is achieved at the (Hopf) bifurcation point where two real roots of (14) turn into a complex conjugate pair.

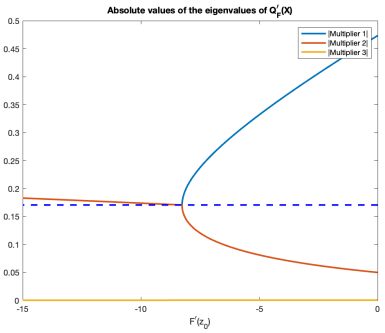

Fig. 3. Absolute values of the eigenvalues of $Q'_F(X)$ as function of $F'(z_0)$. The minimal spectral radius is depicted by dashed line.

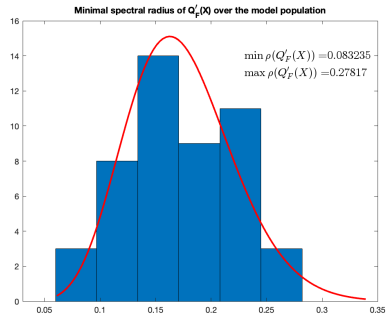

Fig. 4. Histogram of minimal spectral radii of $Q'_F(X)$ over the NMB model population. An approximation with Beta distribution is provided for reference.

b) Phase modulation: Similarly to the case of pure amplitude modulation above, consider

$$Q'_\Phi(X) = \mathrm{e}^{AT} + \Phi'(z_0)DC.$$

This type of impulsive feedback is obtained from (4) by assuming $F(z_0) \equiv \lambda$. The slope of the frequency modulation function has to be positive in order to enforce sparser drug administration intervals for an elevated output. A faster convergence is achieved by the impulsive feedback before the Hopf bifurcation occurs and complex values of the multipliers arise, Fig. 5.

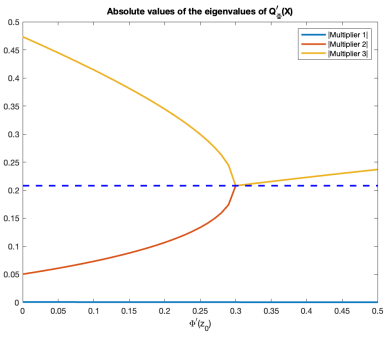

Fig. 5. Absolute values of the eigenvalues of $Q'_\Phi(X)$ as function of $\Phi'(z_0)$. The population mean value is assumed for α. The minimal spectral radius is depicted by dashed line.

c) Amplitude and phase modulation: The convergence to the desired 1-cycle, when both amplitude and frequency modulation are exploited in closed-loop system (3), (4), is difficult to analyze analytically. In Fig. 6, the spectral radius of $Q'(X)$ is calculated for the values of $\Phi'(z_0)$ and $F'(z_0)$ where the multipliers are real. The manifolds where the direct and reverse Hopf bifurcations occur (the edges in blue) are affine functions of $\Phi'(z_0)$ and $F'(z_0)$. This is in line with the stability border observed in Fig. 2 and a direct consequence of the Jacobian being an affine matrix function on the modulation functions slopes, cf. (10). Obviously, the multipliers are always real for $\Phi'(z_0) = F'(z_0) = 0$. When $F'(z_0)$ decreases from zero to some negative value, lower values of $\Phi'(z_0)$ are are required to preserve fixed point stability and improve convergence without giving rise to oscillating transients. Quite soon, when $F'(z_0) < -8.3$, the use of amplitude modulation definitely results in complex multipliers.

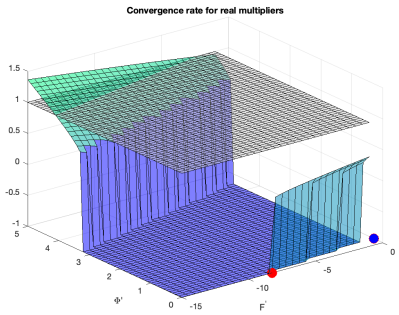

Fig. 6. Spectral radius of $Q'(X)$ as function of $\Phi'(z_0)$ and $F'(z_0)$. Green and light blue surfaces – spectral radius of the Jacobian when all the multipliers are real. Spectral radius is assigned a value of -1 when there are complex multipliers (dark blue area). Grey plane – stability border. Red circle – the optimal value $F'(z_0) = -8.2600$ (only amplitude modulation) for the population mean α. Blue circle – the optimal value $\Phi'(z_0) = 0.29$ (only frequency modulation) for the population mean α.

D. Modulation functions

Following [16], select the controller modulation functions as piecewise affine, i.e.

$$\bar{\Phi}(\xi) = \begin{cases} \Phi_2 & \Phi_2 < k_2\xi + k_1, \\ k_2\xi + k_1 & \Phi_1 \le k_2\xi + k_1 \le \Phi_2, \\ \Phi_1 & k_2\xi + k_1 < \Phi_1, \end{cases}$$

$$\bar{F}(\xi) = \begin{cases} F_1 & k_4\xi + k_3 < F_1, \\ k_4\xi + k_3 & F_1 \le k_4\xi + k_3 \le F_2, \\ F_2 & F_2 < k_4\xi + k_3. \end{cases}$$

Recalling from (2) that $y(t) \in [0, 100]$, the following inequalities apply

$$\Phi_1 \le k_1,\ 100k_2 + k_1 \le \Phi_2,\ F_1 \le k_3,\ 100k_4 + k_3 \le F_2. \tag{15}$$

From the bounds on the modulation functions, it follows that the feedback cannot administer a dose that is greater than F_2 or lower than F_1. Further, no dose is administered sooner than Φ_1 after the previous one and at least one dose is administered within a time interval of Φ_1. These bounds can thus be easily obtained by inspection of the manual medication protocols for the drug in question.

VII. Simulation example

Consider a 1-cycle in closed-loop system (1), (2), (4) with 300 mg of atracurium administered each 20 min (i.e. $\lambda = 300, T = 20$) and, for the population mean values of α, β, design a pulse-modulated controller that sustains this periodic solution.

The fixed point of the desired 1-cycle is given by (13)

$$X^\top = \begin{bmatrix} 269.5974 & 84.5819 & 13.6249 \end{bmatrix}.$$

A periodic solution corresponding to this fixed point is depicted in Fig 7. The corridor in which the periodic solution evolves can be computed without performing a simulation by evoking Proposition 2 in [16]. Notably, the solution in question is a result of driving Wiener system (1), (2) by a train of equidistant impulses, essentially without any feedback involved.

For $F'(\cdot)$ and $\Phi'(\cdot)$ obeying (15), by applying the chain rule, one has

$$\begin{aligned} F'(\bar{y}_0) &= \bar{F}'(\bar{y}_0)\varphi'(\bar{y}_0) = k_4\varphi'(\bar{y}_0), \\ \Phi'(\bar{y}_0) &= \bar{\Phi}'(\bar{y}_0)\varphi'(\bar{y}_0) = k_2\varphi'(\bar{y}_0), \end{aligned} \tag{16}$$

where $\bar{y}_0 = CX$ and

$$\varphi'(\xi) = -\frac{\gamma 100 C_{50}^{\gamma}\xi^{\gamma-1}}{\left(C_{50}^{\gamma} + \xi^{\gamma}\right)^2}.$$

This yields the numerical values $\bar{y}_0 = 13.6249$, $\varphi'(\bar{y}_0) = -0.4073$. To obtain a 1-cycle with the desired parameters, the following equations have to hold

$$\begin{aligned} F(\bar{y}_0) &= (\bar{F} \circ \varphi)(\bar{y}_0) = k_4\varphi(\bar{y}_0) + k_3 = \lambda, \\ \Phi(\bar{y}_0) &= (\bar{\Phi} \circ \varphi)(\bar{y}_0) = k_2\varphi(\bar{y}_0) + k_1 = T. \end{aligned} \tag{17}$$

With the help of Fig. 6 and for the desired 1-cycle, select three sets of values of $F'(\cdot)$, $\Phi'(\cdot)$ to illustrate the impact of the pulse modulation feedback design degrees of freedom. The slope of the amplitude modulation function is kept the same, implying that k_3 and k_4 do not change across the cases.

1) $F'(\bar{y}_0) = -0.1$ and $\Phi'(\bar{y}_0) = 0.29$ are well in an area where the Jacobian has real stable multipliers and possesses the eigenvalues spectrum

   $$\sigma(Q) = \{0.2348, 0.1814, 0.0003\},\ \rho(Q) = 0.23485.$$

   From (16), (17), it follows then $k_1 = 21.5133$, $k_2 = -0.7119$, $k_3 = 299.4782$, $k_4 = 0.2455$.
2) Now the slope of the frequency modulation function is increased. For $F'(\bar{y}_0) = -0.1$ and $\Phi'(\bar{y}_0) = 0.35$, two multipliers turn into a complex conjugate pair and define the spectral radius of the Jacobian

   $$\sigma(Q) = \{0.1972 \pm 0.0870i, 0.0003\},\ \rho(Q) = 0.21554.$$

The coefficients of the frequency modulation function are $k_1 = 21.8264$, $k_2 = -0.8592$.

3) With a further increase in the frequency modulation function slope, $F'(\bar{y}_0) = -0.1$ and $\Phi'(\bar{y}_0) = 0.4$, the imaginary parts of the complex multiplier pair grow, as does the spectral radius of the Jacobian

$$\sigma(Q) = \{0.1881 \pm 0.1195i, 0.0002\},\ \rho(Q) = 0.22288,$$

and $k_1 = 22.0873$, $k_2 = -0.9820$.

Now, the impulsive controller is completely defined and its closed-loop dynamics can be simulated, see Fig. 8. The transients in the beginning of the initial condition responses are identical since the modulation functions saturate at the same level. This a desirable safety feature that otherwise takes a model-predictive controller to be properly ensured. In Case 1, with the real multipliers, the convergence to the 1-cycle is slower than for the other cases, but does not exhibit an overshoot, i.e. overdosing (crossing the lower corridor boundary). By allowing complex multipliers with small imaginary parts, as in Case 2, a faster convergence and a smaller spectral radius are achieved, while the overshoot is hardly noticeable. When the imaginary parts of the complex multipliers become comparable in magnitude with the real parts, the overshoot is clearly observed. Yet, it is probably still acceptable since the plant output (NMB effect) enters the desired corridor and causes the onset of NMB faster in all other considered cases. This is despite the fact that the spectral radius of the Jacobian in Case 3 is higher than in Case 2. Notice also that the controller tends to produce an overshoot about 40min into the NMB procedure.

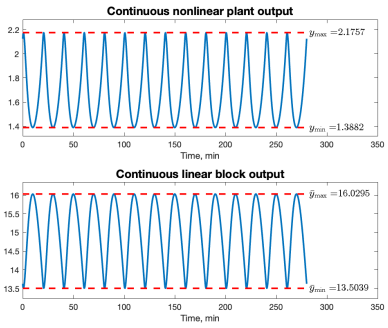

Fig. 7. The designed 1-cycle initiated from the fixed point X. The nonlinear output $y(t)$ (top plot) and the linear output $\bar{y}(t)$ (bottom plot) are presented.

VIII. Conclusions

A pulse-modulated feedback controller is applied to a dosing problem of neuromuscular blocking agent. The proposed controller design method is based on the stabilization of the fixed point of a discrete map describing the evolution of the state vector of the continuous plant from an impulsive control action instant to the next one. Stability of the fixed point guarantees the existence of a basin of attraction along the stationary trajectory where the perturbed closed-loop system solution converges to the stationary one. The convergence rate is assigned by the slopes of the amplitude and frequency modulation functions of the impulsive controller.

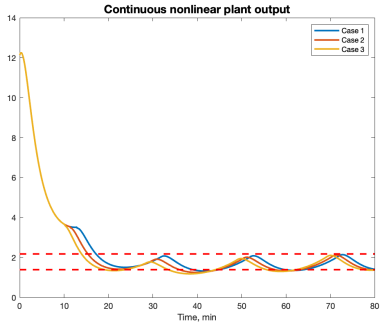

Fig. 8. Transient process to the 1-cycle for three combinations of modulation functions slopes. Case 1: $F'(\bar{y}_0) = -0.1, \Phi'(\bar{y}_0) = 0.29$; Case 2: $F'(\bar{y}_0) = -0.1, \Phi'(\bar{y}_0) = 0.35$; Case 3: $F'(\bar{y}_0) = -0.1, \Phi'(\bar{y}_0) = 0.4$.

References

[1] A. K. Gelig and A. N. Churilov, *Stability and Oscillations of Nonlinear Pulse-modulated Systems*. Boston: Birkhäuser, 1998.

[2] J. Alford and G. Hida, "Discrete systems in process control," *AIChE CEP magazine*, pp. 57–63, June 2022.

[3] R. Bellman, "Topics in pharmacokinetics, iii: Repeated dosage and impulse control," *Mathematical Biosciences*, vol. 12, no. 1, pp. 1–5, 1971.

[4] P. Sopasakis, P. Patrinos, H. Sarimveis, and A. Bemporad, "Model predictive control for linear impulsive systems," *IEEE Transactions on Automatic Control*, vol. 60, no. 8, pp. 2277–2282, 2015.

[5] K. Polonsky, B. D. Given, and E. Van Cauter, "Twenty-four-hour profiles and pulsatile patterns of insulin secretion in normal and obese subjects," *J Clin Invest.*, vol. 81, pp. 442–448, February 1988.

[6] P. S. Rivadeneira, J. Godoy, J. Sereno, P. Abuin, A. Ferramosca, and A. González, "Impulsive MPC schemes for biomedical processes: Application to type 1 diabetes," in *Control Applications for Biomedical Engineering Systems*, A. T. Azar, Ed. Academic Press, 2020, pp. 55–87.

[7] A. Medvedev, A. V. Proskurnikov, and Z. T. Zhusubaliyev, "Design of the impulsive Goodwin's oscillator: A case study," in *American Control Conference*, San Diego, CA, 2023.

[8] ——, "Design of the impulsive Goodwin's oscillator in 1-cycle," in *Proceedings of IFAC World Congress*, Yokohama, Japan, 2023.

[9] M. M. da Silva, T. Wigren, and T. Mendonca, "Nonlinear identification of a minimal neuromuscular blockade model in anesthesia," *IEEE Transactions on Control Systems Technology*, vol. 20, no. 1, pp. 181–188, 2012.

[10] A. Medvedev, A. Churilov, and A. Shepeljavyi, "Mathematical models of testosterone regulation," in *Stochastic optimization in informatics*. Saint Petersburg State University, 2006, no. 2, pp. 147–158, in Russian.

[11] A. Churilov, A. Medvedev, and A. Shepeljavyi, "Mathematical model of non-basal testosterone regulation in the male by pulse modulated feedback," *Automatica*, vol. 45, no. 1, pp. 78–85, 2009.

[12] Z. T. Zhusubaliyev and E. Mosekilde, *Bifurcations and Chaos in Piecewise-Smooth Dynamical Systems*. World Scientific, 2003.

[13] A. V. Proskurnikov, H. Runvik, and A. Medvedev, "Cycles in impulsive Goodwin's oscillators of arbitrary order," *Automatica*, vol. 159, January 2024, article 111379.

[14] Z. T. Zhusubaliyev, A. Churilov, and A. Medvedev, "Bifurcation phenomena in an impulsive model of non-basal testosterone regulation," *Chaos*, vol. 22, no. 1, pp. 013 121–1—013 121–11, 2012.

[15] M. L. Overton and R. S. Womersley, "On minimizing the special radius of a nonsymmetric matrix function: Optimality conditions and duality theory," *SIAM Journal on Matrix Analysis and Applications*, vol. 9, no. 4, pp. 473–498, 1988.

[16] A. Medvedev, A. V. Proskurnikov, and Z. T. Zhusubaliyev, "Output corridor control via design of impulsive Goodwin's oscillator," in *American Control Conference*, Toronto, Canada, 2024.